Research Square

Preprints are preliminary reports that have not undergone peer review.
They should not be considered conclusive, used to inform clinical practice,
or referenced by the media as validated information.

High-Accuracy Method for Measuring the Specific Heat Capacity of Molten Salts: Application to the FLiNaK and NaCl-MgCl2 Eutectics

Juliano Schorne-Pinto
julianos@mailbox.sc.edu
University of South Carolina
Aiswarya Padinhare Manissery
University of South Carolina
Ronald E. Booth
University of South Carolina
Annabelle Husek
University of South Carolina
Zachary K. Gardiner
University of South Carolina
Jorge Paz Saldan Palma
University of South Carolina
Jacob A. Yingling
Idaho National Laboratory, Idaho Falls
Theodore M. Besmann
University of South Carolina

Research Article

Keywords: Heat capacity, molten salts, eutectic, FLiNaK, NaCl-MgCl2, DSC, Calvet calorimetry, crucible design

Posted Date: April 24th, 2026

DOI: https://doi.org/10.21203/rs.3.rs-9431226/v1

License: This work is licensed under a Creative Commons Attribution 4.0 International License.
Read Full License

Additional Declarations: No competing interests reported.

Version of Record: A version of this preprint was published at International Journal of Thermophysics on July 11th, 2026. See the published version at https://doi.org/10.1007/s10765-026-03805-8.

High-Accuracy Method for Measuring the Specific Heat Capacity of Molten Salts: Application to the FLiNaK and NaCl-$MgCl_2$ Eutectics

Juliano Schorne-Pinto[1*], Aiswarya Padinhare Manissery[1], Ronald E. Booth[1], Annabelle Husek[1], Zachary Gardiner[1], Jorge Paz Saldan Palma[1], Jacob A. Yingling[2], and Theodore M. Besmann[1]

[1] Nuclear Engineering Program, Department of Mechanical Engineering, University of South Carolina, Columbia, SC 29208, USA

[2] Advanced Technology of Molten Salts Department, Idaho National Laboratory, Idaho Falls, ID 83415, USA

*Corresponding author: julianos@mailbox.sc.edu (Juliano Schorne-Pinto).

Abstract:

Specific heat values for molten salts are essential for thermal-hydraulic analysis, reactor physics calculations, and thermochemical modeling of molten salt reactors. However, achieving reduced measurement uncertainty requires rigorous control of experimental conditions, high-precision calorimetric instrumentation, and a maximized sample-to-crucible mass ratio. This study presents a procedure for high-accuracy measurement of the specific heat (c_P) of air-sensitive molten salts using a Calvet-type DSC with a small temperature step method and custom laser-welded lightweight hermetic nickel crucibles. Instrument reproducibility of 1.54% (k = 2) was achieved and validated through independent triplicate measurements of a NIST SRM720 sapphire standard. Using this methodology, the c_P of molten 46.5LiF-11.5NaF-42KF mol% (FLiNaK) and 58NaCl-42$MgCl_2$ mol% (NaCl-$MgCl_2$) eutectics was determined with expanded uncertainties (k = 2) of 1.74% and 1.93%, respectively, for high-purity samples, incorporating regression contributions. These results confirm previously reported positive excess heat capacities in both eutectics, with an improved description of the temperature dependence. The measured data provide reference values for the Molten Salt Database - Thermochemical, and the protocol is readily transferable to other molten salts, including actinide-bearing fuel salts.

Keywords: Heat capacity, molten salts, eutectic, FLiNaK, NaCl-$MgCl_2$, DSC, Calvet calorimetry, crucible design

1 Introduction:

Growing interest in heat transfer fluids (HTFs) [1, 2], thermal storage media [2], and molten salt reactor (MSR) fuels and coolants [3] is driving renewed research into the thermophysical and thermochemical properties of molten salt systems. In this context, the *Molten Salt Database – Thermochemical* (MSD-TC), previously the *Molten Salt Thermal Properties Database – Thermochemical* (MSTDB-TC) [4–6] and its companion, the *Molten Salt Database – Thermophysical* (MSD-TP) [7, 8] are being developed as key resources for evaluated properties of molten salt mixtures relevant to MSRs. As part of this endeavor, critical measurements for molten-salt coolants and fuels are being generated for inclusion in the databases to address knowledge gaps and validate historical datasets for use in reactor design, safety analysis, and materials qualification.

Among the various thermophysical properties of molten salts, the heat capacity (C_P) or specific heat capacity (c_P) is critical for heat-transfer calculations and is directly related to the second derivative of Gibbs energy, playing a major role in CALPHAD-type modeling [9]. Accurate c_P data are needed for thermal-hydraulic codes used in reactor safety analysis, where uncertainties propagate directly to predicted temperature profiles and safety margins. Despite decades of research, significant uncertainty persists among reported c_P values for molten salts. For example, literature values for the c_P of the FLiNaK eutectic (46.5LiF-11.5NaF-42KF mol%) range from 1.45 to 2.35 $J.g^{-1}.K^{-1}$ [10–25], a span of nearly 61% (**Figure 1**a,b).

Conventional heat-flux differential scanning calorimeters (HF-DSCs) are the most widely used instruments to determine the c_P of materials, including liquids. However, even under carefully optimized protocols, reported uncertainties for liquids often remain in the 5–10% range and may, in practice, be underestimated. The HF-DSC datasets of **Figure 1**a show that those with similarly reported uncertainties [11–13, 15–19, 21, 22] for FLiNaK may differ by 30%. Several factors contribute to limiting accuracy, including salt-crucible incompatibility, inadequate crucible geometry, atmospheric contamination during salt synthesis, handling or measurement, and irreproducible thermal contact between the crucible and the thermocouple resulting in baseline drift. At higher temperatures and the aggressive chemistries encountered with fluoride- and chloride-based salts, commercial crucibles fail to provide both hermetic sealing and chemical inertness, with the notable exception of hermetically sealed gold crucibles [26]. Glassy carbon crucibles [27] are stable with respect to salts and useful if the instrument is operated inside an inert-gas glovebox to prevent sample contamination from atmospheric gases, since glassy carbon crucibles cannot be hermetically sealed. Customized nickel liners have also been successfully utilized in sealed stainless-steel Netzsch crucibles [28] to prevent salt-crucible interactions. However, the reduced sample-to-crucible mass ratio and the difficulty of achieving reproducible thermal contact between the liner and the crucible are significant challenges [17].

As other approaches, relatively accurate c_P values with reported uncertainties of approximately 2-5% can be obtained by modulated DSC (MDSC) [29] and power-compensated DSC (PC-DSC)

[10]. In MDSC, a sinusoidal temperature modulation superimposed on linear heating enables direct c_P calculation from the reversing heat flow signal without the need for a separate reference material run [29]. On the other hand, PC-DSC maintains equal temperature between two separate micro-furnaces (each with independent heaters and temperature sensors) by adjusting electrical power supplied to each, with the heat flow inferred directly from the power difference. Two studies used MDSC measurements for FLiNaK [18, 20], with another using PC-DSC [10], with all reporting dissimilar results (**Figure 1**b).

Drop calorimetry offers an alternative approach, with c_P obtained indirectly from enthalpic measurements. Although various drop calorimeters were employed for molten salts in the 1950s–1970s, including three studies of FLiNaK [23] (**Figure 1**b), HF-DSCs subsequently became dominant because of their operational simplicity and higher throughput. Recently, drop calorimetry has seen renewed interest driven by the need for reliable data at higher temperatures (>1000 K). In this context, two types of instruments have been used for molten salts: a twin Calvet high-temperature calorimeter [30, 31] and a pseudo-Calvet calorimeter [32]. Unlike conventional HF-DSC and MDSC instruments, which rely on a planar thermocouple array beneath the sample (i.e., a 2D sensor) sensitive primarily to conductive heat transfer, Calvet-type calorimeters employ a three-dimensional thermopile consisting of dozens to hundreds of thermocouples arranged cylindrically around the sample and reference cells. Nearly all exchanged heat is captured, substantially reducing sensitivity to sample positioning and thermal asymmetries [33]. The twin configuration consists of two cylindrical thermopiles, each containing 128 thermocouples that completely surround the sample and reference within a massive calorimetric block, whereas the pseudo-Calvet type uses a reduced number of thermocouples in a single cylindrical thermopile [33]. Because drop calorimetry measurements are typically carried out over wide temperature ranges, yielding large enthalpy increments, the c_P values derived by differentiation of the enthalpy-temperature curve are sensitive to data scatter, regression quality, and degree of the fit polynomial, with reported uncertainties typically in the 3–10% range. As an alternative to drop mode operation, Calvet-type DSC (also known as Tian-Calvet DSC) operated in scanning mode combines the operational flexibility of HF-DSC with the improved heat-flow measurement precision and sensitivity provided by a three-dimensional thermopile.

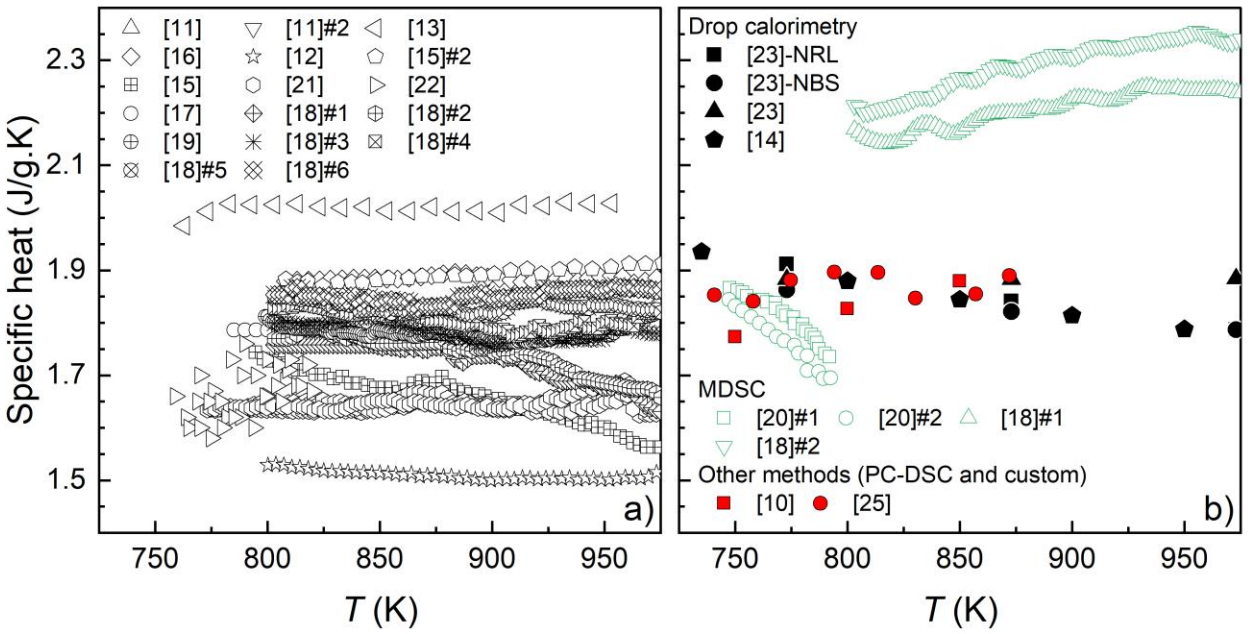


Figure 1: Compiled data for the specific heat of FLiNaK from literature sources, illustrating the significant scatter among datasets despite similar reported uncertainties. a) HF-DSC [11–13, 15–19, 21, 22]**,** and b) Drop-calorimetry [14, 23], MDSC [18, 20], and other methods [10, 25].

This work employs a Calvet DSC to obtain high-accuracy c_P data for two relevant eutectic molten salts: FLiNaK and 58NaCl-42$MgCl_2$. The FLiNaK composition is commonly used as a surrogate for FLiBe (2LiF-BeF_2) due to its similar thermophysical behavior that allows measurements to be made without dealing with toxic beryllium. The 58NaCl-42$MgCl_2$ eutectic is of interest as a coolant and solvent for uranium and transuranic elements (Pu, Np, Am, and Cm). Accurate thermophysical properties for both eutectics are essential to address current knowledge gaps and refine existing property values that still exhibit a wide spread in reported uncertainties. Because such legacy data persist in design databases for decades, a procedure for high-accuracy c_P measurement with rigorously quantified uncertainty is presented.

2 Materials and Methods:

2.1 Materials:

High-purity NaCl (AnhydroBeads^{TM} 99.999%, Millipore-Sigma, USA) was pre-melted with tantalum scraps to reduce the oxygen content. Anhydrous $MgCl_2$ (99.99%, Thermo Fisher Scientific, USA) was used as received with the purified NaCl to prepare the 58NaCl-42$MgCl_2$ eutectic. The FLiNaK sample material was obtained from Oak Ridge National Laboratory (ORNL) [26].

2.2 Sample Preparation:

All samples were prepared in a low-oxygen, low-moisture MBraun Unilab Pro glovebox under high purity argon (Linde, >99.999%), with oxygen content below 1 ppm and moisture content

maintained below 0.1 ppm. Salts and crucibles were weighed using a Mettler Toledo XPR105 semi-micro balance, for which an expanded uncertainty U of 0.02 mg was determined using **Eq. 1** with Y as the certified weights (**Table S1**), following the Guide to the Expression of Uncertainty of Measurement (GUM) [34].

$$U = t_{N-1;\,95\%} \sqrt{\frac{1}{N-1}\sum_{i=1}^{n}[Y_{measured} - Y]^2} \qquad \text{Eq. 1}$$

where $Y_{measured}$ is the experimental value measured, N is the sample size, and $t_{N-1;\,95\%}$ is the Student's t-factor for a two-tailed distribution at 95% confidence (p = 0.95) for $N - 1$,

2.3 Oxygen Content Analysis:

Oxygen content was determined by an inert gas fusion (IGF, Eltra Elementrac OH p-2 analyzer, USA). Salt samples were ground to a powder, packed, and crimp-sealed in tin capsules within an inert glovebox prior to removal and introduction into the IGF furnace, details are provided in [35]. Multiple samples of each salt were measured to establish measurement uncertainty, calculated using **Eq. 1**, where Y is the mean value of the measurements, yielding NaCl (58 ± 31 wppm, N = 3), $MgCl_2$ (42 ± 20 wppm, N = 6), FLiNaK (117 ± 25 wppm, N = 13). Further details are provided in **Table S2**.

2.4 Apparatus:

A Calvet-type DSC (Calvet Pro, Setaram, Caluire-et-Cuire, France) was used to obtain highly accurate thermal measurements. It was factory-calibrated using the Joule effect, with an operational temperature range of 293–1103 K. This instrument is equipped with two 3D thermopiles, each containing 120 thermocouples arranged in 10 concentric rings, offering maximum precision and sensitivity for heat-flow measurement. The thermopiles region has a practical length of 10–12 mm and an inner diameter of 7 mm. A removable custom-made quartz tube liner (6.9 mm outer diameter, 5 mm inner diameter) was employed to protect the thermocouples from potential leaking or volatilization of the salts. These quartz tubes were marked to indicate their radial position, ensuring reproducible placement inside the calorimeter.

2.5 Development of a Laser-Welded, Smooth-Wall Nickel Crucible for Molten-Salt c_P Measurements:

Due to the limited dimensions of the measurement region in the calorimeter and the high chemical reactivity of the molten samples, none of the commercially available crucible options were suitable. Moreover, our instrument is installed outside a glovebox, necessitating the use of hermetically sealed crucibles to avoid exposure of salt to air and moisture. These issues are not unique to our setup, as illustrated by the pioneering work of Gaune-Escard and co-workers [36–39], who measured c_P of solid and liquid salts using custom hermetically sealed quartz cells with

a similar Calvet calorimeter. Quartz crucibles were not considered in the present work because the crucible material must be chemically compatible with both chloride- and fluoride-based salts.

A nickel crucible design for fluoride-based salt drop calorimetry was previously reported [32] for use in a pseudo-Calvet-type calorimeter installed inside a glovebox at the Joint Research Centre (JRC) Karlsruhe. Inspired by this approach, a custom nickel crucible was specifically designed and fabricated for the Calvet DSC used in this work, to maximize the sample-to-crucible mass ratio while maintaining a highly symmetric cylindrical geometry (**Figure 2**a,b).

Consistent crucible mass achieved by selecting crucibles with mass values within 0.2 mg and then polishing the surfaces to achieve a mass difference within ± 0.02 mg. Nickel crucible lids were custom-made such that they fit tightly onto the crucibles and were also polished to match within ± 0.02 mg. A custom-made tool was used to press the lid into the crucible within the controlled atmosphere of the glovebox. A Nd:YAG 1064 nm laser was then used to weld the crucibles at a frequency of 10 Hz with a spot diameter of 0.3 mm (**Figure 2**c). The crucible was placed inside a stainless-steel heat sink (**Figure 2**d) protected with tantalum shielding to prevent welding to the heat sink. The assembly was rotated at $10°.s^{-1}$ using a motorized rotation stage (**Figure 2**d), programmed to execute three full rotations to ensure adequate sealing.

The effectiveness of welding was validated using both FLiNaK and 58NaCl-42$MgCl_2$ samples where sealed crucibles were positioned horizontally within a fused silica crucible and heated to 1123 K for one hour in a furnace located in an inert glovebox. The internal pressure was estimated to be less than 0.4 MPa at this temperature, and the vapor pressures of both salts were calculated to be below 100 Pa. Any signs of leakage, such as changes in mass or discoloration of the crucible or surrounding area, were used to identify failed specimens, with three of four crucibles passing the leak test.

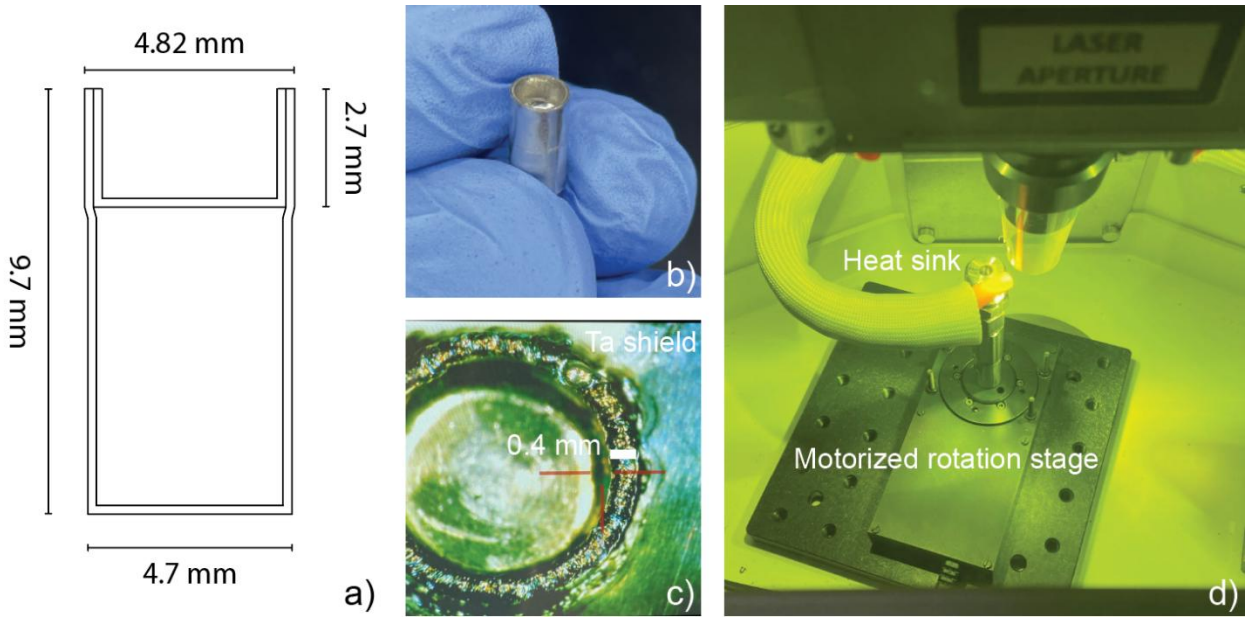


Figure 2: a) Schematic of the nickel crucible design. b) Photograph of the mechanically sealed crucible prior to welding. c) Photograph of the laser guide and the welded area. d) Motorized rotation stage with a heat sink.

2.6 Temperature Calibration:

A four-point temperature calibration was performed using individual indium (429.748 K, Netzsch calibrant), lead (600.612 K, ≥99.999%, Thermo Scientific Chemicals, USA), zinc (692.677 K, Netzsch calibrant), and antimony (903.778 K, 99.9999%, BeanTown Chemical, USA) calibrants encapsulated in flame-sealed quartz ampules. The calibration followed the zero-heating rate method [40], in which calibrants experience heating rates varying by at least a factor of 10 (here β = 16, 8, 4, 1.6 K.min^{-1}), with the onset temperatures extrapolated to a zero-heating rate to obtain a true melting temperature.

Encapsulated FLiNaK samples were used to verify the accuracy of the temperature and sensitivity calibrations (**Table 1**), with the first melting cycle discarded, and an overall uncertainty in temperature of ± 2 K assumed. Although the instrument exhibits high intrinsic precision as shown in **Table 1** (i.e., ± 0.2K), the use of different crucible types for the temperature calibration and for c_P measurements introduces additional systematic uncertainty.

Table 1: Experimental FLiNaK melting temperatures using current calibration. The uncertainty* is calculated using **Eq. 1** and $t_{N-1;\,95\%}$ is equal to 3.18 for $p = 0.95$.

Rate	Cycle 2	Cycle 3	Cycle 4	Cycle 5	Average	Uncertainty*
K.min^{-1}	K	K	K	K	K	K
4	731.9	731.8	732.1	732.0	732.0	0.2
K.min^{-1}	J.mol^{-1}	J.mol^{-1}	J.mol^{-1}	J.mol^{-1}	J.mol^{-1}	J.mol^{-1}
4	16,565	16,641	16,704	16,633	16,636	90

* Derived from the measurements themselves and here listed to show the precision of the measurements.

The melting point of 732.0 ± 2 K is in relatively good agreement with our previous result of 733.8 ± 2.3 K [17]. The enthalpy of fusion of 16,636 ± 90 J.mol^{-1} agrees well with PC-DSC results from Rogers *et al.* [10] (16,646 ± 333 J.mol^{-1}, $N = 27$ runs).

2.7 Measurement Procedure

Measurements were made using the discontinuous small temperature step method [36, 41–43] to reduce the influence of baseline drift, albeit at the cost of longer measurement times, in conjunction with a three-step (zero-line/reference/sample) methodology [41]. The first step, i.e., the zero-line measurement, was performed using identical, empty crucibles for the sample and reference under an argon flow of 5.75 mL.min^{-1} and the same temperature program as all subsequent measurements, thereby removing any effect of instrumental asymmetry. The reference crucible was retained for all subsequent measurements. The second step is the calibration measurement using a well-defined reference material, which in this case was the NIST Standard Reference Material SRM720, a cylindrical sapphire (α-Al_2O_3) single crystal specimen 71.80 ± 0.02 mg in mass. The third step is measurement of a pre-melted sample that had been leak tested. The

temperature program parameters involved step increments of 5 or 10 K, a heating rate of 1.5 K.min^{-1} between steps, and a stabilization time of 800 s after each step to attain steady-state conditions. **Figure 3**a illustrates representative signals from calibration and measurement steps after subtracting the zero-line correction.

Values for c_P were obtained from just above the melting point to temperatures 30–130 K higher using the small temperature steps method. Measurements were performed on consecutive days to minimize calibration drift, with a complete instrument restart and full recalibration performed between sample sets. This protocol ensured that each sample set was referenced to an independent calibration, enabling assessment of reproducibility. The resulting data were used for a type A uncertainty evaluation of the instrument [34].

The specific heat ($c_P(\bar{T})$) of the salt was determined using **Eq. 2**,

$$c_P(\bar{T}) = \left[\frac{Q_{\bar{T}}}{\Delta T \cdot m_{sample} \cdot S_{\bar{T}}}\right]_{Sample} + \left[\frac{\frac{(m_{cr,ref} - m_{cr,sample})}{m_{sample}} \cdot c_P(\bar{T})_{Nickel}}{S_{\bar{T}}}\right]_{Correction} \quad \text{Eq. 2}$$

where $S_{\bar{T}}$ represents the calibration factor (sensitivity) obtained from the instrument calibration at $\bar{T}$ (average temperature of the step), $Q_{\bar{T}}$ denotes the difference in integrated area between the sample and the zero-line profile, ΔT is the temperature interval of the small step, $m_{cr,ref}$ denotes the mass of the reference crucible, $m_{cr,sample}$ is the mass of the crucible containing the sample, and m_{sample} is the mass of the sample. Mass losses incurred during the welding process were accounted for in the second term of **Eq. 1** in a manner analogous to that described by Höhne *et al.* [41] The $c_P(\bar{T})_{Nickel}$ is known with sufficient accuracy and obtained from the thermodynamic database of the Scientific Group Thermodata Europe (SGTE) [44].

2.8 Determining Measurement Accuracy:

Instrument reproducibility was evaluated by measurements using the calibration reference sapphire sample (SRM720) under three independent calibration cycles, following the same protocol as used for the molten salt measurements. A total of 54 data points were obtained between 745.6 K and 871.7 K (**Figure 3**b) and are seen to cluster closely around the recommended values of Ditmars *et al.* [45] Each point was treated as an independent measurement in order to determine values for the residuals. The residual standard deviation (RSD) was calculated using **Eq. 3**

$$RSD(\%) = t_{N-1;\,95\%} \sqrt{\frac{1}{N}\sum_{i=1}^{n}\left[\frac{Y_{measured} - Y}{Y} \cdot 100\right]^2} \quad \text{Eq. 3}$$

where the reference values [45] are Y, and in this case yield a value of 1.54 %, which was adopted as representative of the determined c_P measurements. This value represents the minimum

uncertainty achievable with the current protocol and accounts for calibration drift, zero-line variability, and day-to-day environmental fluctuations. Contributions from sample and reference mass measurements (± 0.02 mg each; ≤ 0.05% combined), SRM720 certified c_P values (± 0.05% per Archer [46]), and post-measurement crucible oxidation (< 0.02 mg; < 0.007% of ~ 302.4 mg crucible mass) were negligible and were not propagated further.

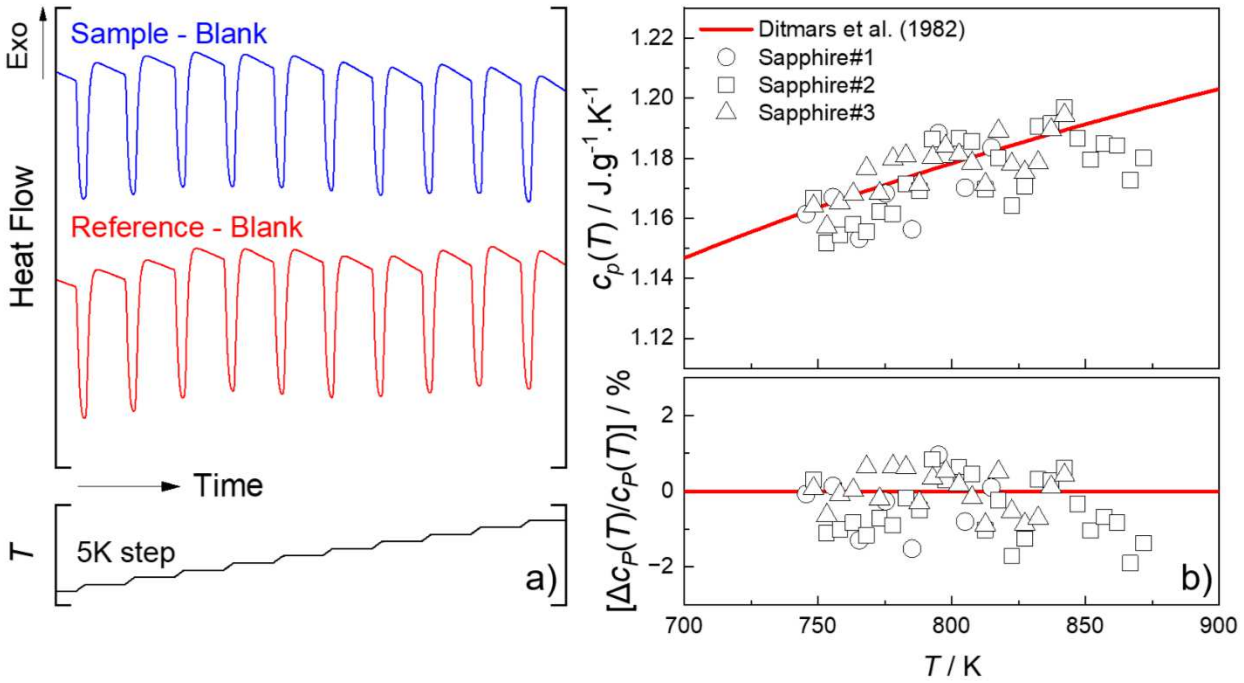


Figure 3: a) Small temperature step method for the determination of c_P with an 800 s isothermal period to allow the system to reach steady-state between steps. b) Measured c_P of sapphire (SRM720) standard compared with the reference values [45] and the corresponding residuals.

3 Results and Discussion

3.1 Specific Heat of Molten FLiNaK

The FLiNaK composition is commonly used to benchmark thermophysical properties, and its c_P has been extensively studied, as summarized in **Figure 1**a,b. Reported c_P values range from 1.45 J.g^{-1}.K^{-1} to 2.35 J.g^{-1}.K^{-1}, with an unweighted average of 1.829 J.g^{-1}.K^{-1} when each dataset was normalized by the number of data points. Here, the c_P was revisited to clarify its temperature dependence as relatively accurate methods such as PC-DSC [10] suggest a positive temperature coefficient, whereas the MDSC determinations of Ambrosek [20] and drop calorimetry data from four independent studies [14, 23] indicate a negative temperature coefficient. In contrast, HF-DSC results generally suggest quasi-constant behavior.

Results from independent sets of measurements on a single FLiNaK sample of 47.08 ± 0.02 mg are listed in **Table 2** and shown in **Figure 4**a. The uncertainty in the fitted c_P relation was determined from

$$U_{fit} = 2\sqrt{\frac{1}{N-m}\sum_{i=1}^{n}\left[\frac{Y_{measured}-Y_{ref}}{Y_{ref}}\cdot 100\right]^2} \quad \text{Eq. 4}$$

where m is the number of coefficients with a Student's t-factor for a two-tailed distribution of 2 as $N = 40$. The overall uncertainty of the c_P is described by **Eq. 5**,

$$U_{total} = \sqrt{RSD^2 + {U_{fit}}^2} \quad \text{Eq. 5}$$

calculated using the determined instrument RSD of 1.54% and the uncertainty in fitting the c_P data, and yielding an extrapolated uncertainty of 1.74% for

$$c_P(J/g.K)_{FLiNaK} = 1.875 - 0.00007808T \quad \text{Eq. 6}$$

A slight negative temperature dependence was identified in the limit of the uncertainty, qualitatively consistent with that seen in drop calorimetry values [14, 23] although they exhibit steeper negative slopes and generally higher c_P values.

Table 2: Specific heat of molten FLiNaK with an extrapolated uncertainty of 1.74%.

Run#1		Run#2		Run#3		Run#3 – continued	
T (K)	**c_P (J/g.K)**	**T (K)**	**c_P (J/g.K)**	**T (K)**	**c_P (J/g.K)**	**T (K)**	**c_P (J/g.K)**
738.4	1.814	755.3	1.824	748.3	1.828	812.6	1.822
743.3	1.809	765.2	1.825	753.3	1.813	817.5	1.807
748.3	1.815	775.1	1.816	758.2	1.825	822.5	1.811
753.3	1.815	785.0	1.824	763.2	1.826	827.4	1.802
758.2	1.804	794.9	1.812	768.1	1.807	832.3	1.800
763.1	1.807	804.8	1.811	773.1	1.812	837.3	1.816
768.1	1.805	814.6	1.805	778.0	1.805	842.2	1.813
				782.9	1.814	847.1	1.809
				787.9	1.816	852.1	1.809
				792.8	1.823	857.0	1.813
				797.8	1.822	861.9	1.804
				802.7	1.803	866.9	1.809
				807.7	1.817	871.8	1.803

A compilation of reported enthalpy increment ($H_T - H_{298.15}$) [14, 23] values are seen in **Figure 4**b compared with the sum of the integral heat capacity of FLiNaK(s) computed using MSD-TC [5, 17], the enthalpy of fusion listed in **Table 1**, and the integral of the heat capacity values of molten FLiNaK from **Eq. 6**, converted to $H_T - H_{298.15}$ using 41.291 g/mol. Very good agreement is illustrated by the residual analysis in **Figure 4**b with the results of Minchenko *et al.* [14] (within

0.26 kJ.mol^{-1}) and those of Powers and Blalock [23] (within 0.75 kJ.mol^{-1}), demonstrating not only the precision of the current measurements but also their consistency with related thermodynamic properties.

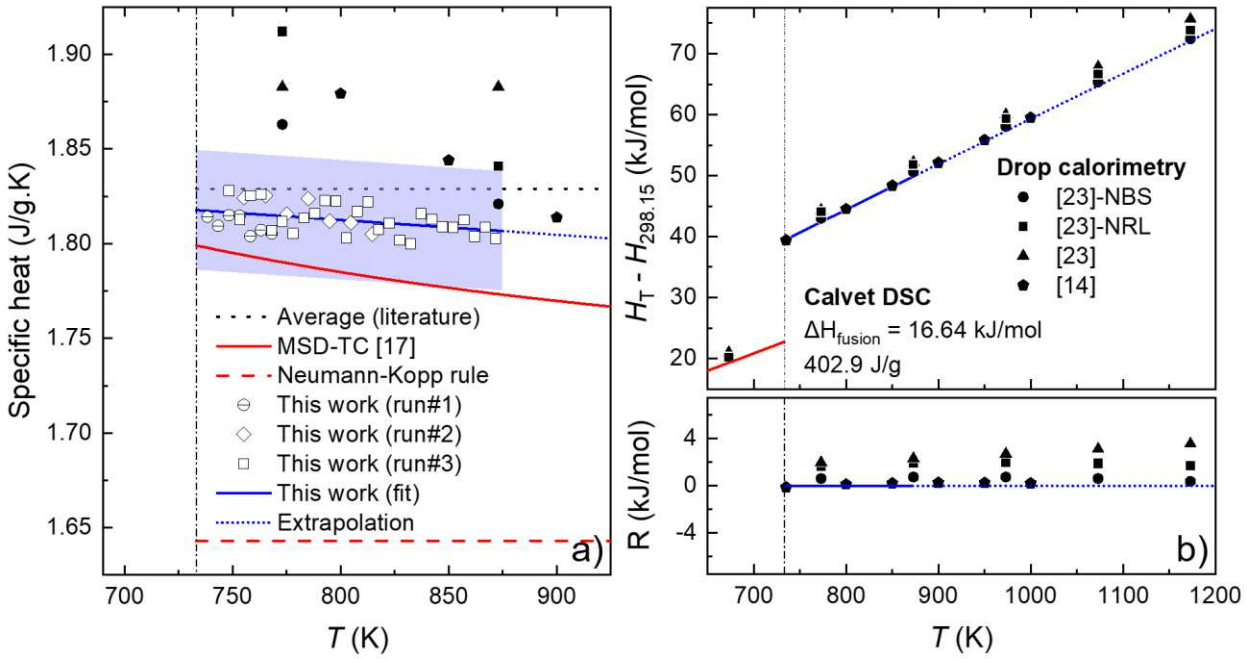


Figure 4: a) Measured c_P of molten FLiNaK compared with those from the Neumann-Koop rule, computed from MSD-TC [5, 17], unweighted average value from available datasets, and indirectly derived drop calorimetry values [14, 23]. b) Reported enthalpy increment for molten FLiNaK[14, 23] compared with the sum of the integrated c_P of FLiNaK(s) from MSD [5, 17], measured enthalpy of fusion, and the heat capacity.

Using the ideal additive Neumann-Kopp rule (NKR), a c_P of 1.643 J.g^{-1}.K^{-1} is estimated for FLiNaK such that the excess specific heat (c_P^{ex}) (defined as the difference between the measured and NKR values), is determined to be 0.175 ± 0.032 J.g^{-1}.K^{-1} at 733 K and 0.164 ± 0.031 J.g^{-1}.K^{-1} at 875 K. These new results can be compared with an independent estimate from reported earlier efforts [17], where the c_P^{ex} was derived from the temperature dependence of the enthalpy of mixing ($\Delta_{mix}H$) of the LiF-NaF and LiF-KF pseudo-binary systems using:

$$c_P^{ex} = \left(\frac{\partial \Delta_{mix} H}{\partial T}\right)_P \qquad \text{Eq. 7}$$

The resulting c_P^{ex} value of these systems was extrapolated to the LiF-NaF-KF system using the CALPHAD method, yielding values of 0.156 ± 0.078 J.g^{-1}.K^{-1} at 733 K and 0.130 ± 0.078 J.g^{-1}.K^{-1} at 875 K. These values agree within the combined uncertainties, providing additional independent validation of the calorimetric results.

3.2 Specific Heat of the Molten 58NaCl-42MgCl$_2$ Eutectic

Reported c_P values derived from drop calorimetry [31, 47, 48] for molten NaCl-$MgCl_2$ near the eutectic composition range from 1.187 J.g^{-1}.K^{-1} to 1.34 J.g^{-1}.K^{-1} (**Figure 5**a). These values were assumed to be temperature-independent within the experimental uncertainties. The only reported HF-DSC study is that of Mohan *et al.* [49] whose values approach those of the NKR following a steep decrease in c_P between the eutectic melting temperature and 775 K. This behavior is inconsistent with the above-noted drop calorimetry data and yields values somewhat lower than following the Dulong-Petit law, warranting further investigation. In addition to the aforementioned values, Williams [50] listed what they termed was a measured value of 0.258 cal.g^{-1}.K^{-1} (i.e., 1.079 J.g^{-1}.K^{-1}) at 973 K and a predicted value of 0.262 cal.g^{-1}.K^{-1} (1.096 J.g^{-1}.K^{-1}), however, the source of the measured value was not identified. Reported c_P values for the similar 38.2NaCl-41.3KCl-20.5$MgCl_2$ eutectic measured by HF-DSC [51, 52] suggest a negative temperature-dependence (**Figure 5**a).

Two samples were prepared of the 58NaCl-42$MgCl_2$ eutectic composition of 58.85 ± 0.02 mg and 73.49 ± 0.02 mg each. The DSC analysis for the first sample used a step temperature of ~10 K between 745.6 K and 804.9 K, with the second using smaller steps of ~5 K between 748.3 K and 871.7 K (**Table 3)**. Regression of the combined datasets yielded the following c_P expression:

$$c_P(J/g.K)_{58NaCl-42MgCl2} = 1.684 - 0.000623106T \quad \text{Eq. 8}$$

with an expanded uncertainty (k = 2) of ±1.93%, including contributions from instrument reproducibility and regression. A negative temperature dependence was thus identified, with a similar slope to that for the 38.2NaCl-41.3KCl-20.5$MgCl_2$ eutectic, and when extrapolated, it has a fortuitous agreement with the tabulated value from Williams [50] at 973 K. The resulting c_P^{ex} equals 0.130 ± 0.024 J.g^{-1}.K^{-1} at 745 K and 0.057 ± 0.022 J.g^{-1}.K^{-1} at 875 K.

Table 3: Specific heat of molten 58NaCl-42$MgCl_2$ with an extrapolated uncertainty of ±1.93%.

58NaCl-42$MgCl_2$ (m = 58.85 mg)				58NaCl-42$MgCl_2$ (m = 73.49 mg)			
T (K)	**c_P (J/g.K)**	**T (K)**	**c_P (J/g.K)**	**T (K)**	**c_P (J/g.K)**	**T (K)**	**c_P (J/g.K)**
745.6	1.228	748.3	1.216	792.8	1.179	837.2	1.166
755.5	1.214	753.3	1.223	797.7	1.192	842.2	1.154
765.4	1.210	758.2	1.207	802.7	1.166	847.1	1.157
775.3	1.203	763.2	1.216	807.6	1.174	852.0	1.161
785.1	1.196	768.1	1.197	812.6	1.166	857.0	1.151
795.0	1.189	773.0	1.208	817.5	1.174	861.9	1.145
804.9	1.179	778.0	1.204	822.4	1.177	866.8	1.154
		782.9	1.189	827.4	1.174	871.7	1.142
		787.9	1.200	832.3	1.159		

The $H_T - H_{298.15}$ values for FLiNaK are shown in **Figure 5**b for the solid and liquid phases near the eutectic composition [31, 47, 48]. These include eleven experimental points graphically

extracted from Markov *et al.* [47], who obtained measurements for the 57NaCl-43$MgCl_2$ composition over 727-973 K (**Figure 5**b), deriving a constant c_P value of 1.187 J.g^{-1}.K^{-1} (**Figure 5**a). Denielou *et al.* [48] also studied this system, and their data were also graphically extracted for measurements on multiple samples proximate to the 60NaCl-40$MgCl_2$. Multiple sources of salts were used, likely contributing to the wide variation in c_P values (**Figure 5**a). Their $H_T - H_{298.15}$ measurements for the solid phase, summarized in **Figure 5**b, disagree with unpublished work carried out by our team using synthesized phase-pure $NaMgCl_3$(s), Na_2MgCl_4(s), and $Na_2Mg_3Cl_8$(s) for which c_P measurements were performed [53]. The computed $H_T - H_{298.15}$ for the solid phases, together with the measured enthalpy of fusion of 274.6 ± 0.4 J.g^{-1} and integrated molten phase c_P of **Eq. 8**, yielded $H_T - H_{298.15}$ values at the 58NaCl-42$MgCl_2$ composition of the current effort. As would be expected, the values fall between those for the 57NaCl-43$MgCl_2$ composition of Markov *et al.* [47] and those for the 60NaCl-40$MgCl_2$ compositions of Denielou *et al.* [48] (**Figure 5**b). Both datasets are captured within ± 1.5 kJ.mol^{-1}, as illustrated by the residual analysis. The reported $H_T - H_{298.15}$ values of Strzelecki *et al.* [31] significantly deviate from those of others, possibly due to samples being inadequately equilibrated.

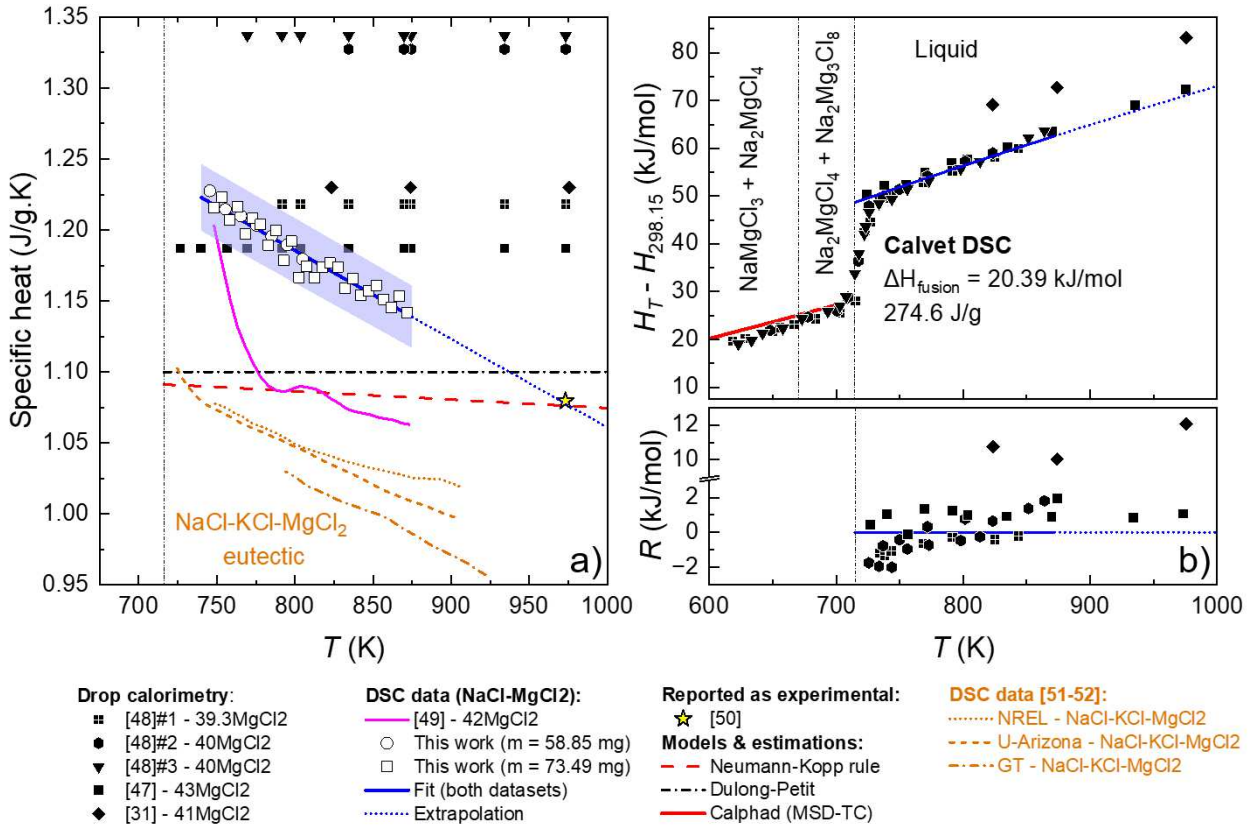


Figure 5: a) Measured c_P of molten NaCl-$MgCl_2$ mixtures proximate to the eutectic composition and of the 38.2NaCl-41.3KCl-20.5$MgCl_2$ eutectic. b) Reported $H_T - H_{298.15}$ as well as values determined from current and earlier work for 58NaCl-42$MgCl_2$(s).

4 Conclusions

A high-accuracy methodology for measuring the c_P of air-sensitive molten salts has been developed using a Calvet-type DSC using the small temperature step method. Custom, lightweight, laser-welded, hermetic nickel crucibles were designed to address the lack of commercially available crucibles appropriate to the 3D thermopile array of the Calvet-type DSC. Instrument reproducibility of 1.54% ($k = 2$) was validated through triplicate measurements a sapphire standard (NIST-SRM 720).

The methodology was applied to two eutectic molten salts relevant to advanced nuclear systems: FLiNaK and 58NaCl-42$MgCl_2$. Measurements were performed over 745–872 K, yielding values with expanded uncertainties ($k = 2$) of 1.74% and 1.93%, for the respective compositions, where the these included contributions from instrument reproducibility and the regression analysis. The uncertainties represent a substantial improvement over those inherent to conventional HF-DSC determinations (typically 5-10%) and to drop calorimetry (3-10%), now allowing sufficient precision to resolve subtle temperature dependencies in the behavior of the c_P of molten salts. A small negative temperature dependence was seen in the c_P for molten FLiNaK, in qualitative agreement with reported values from drop calorimetry. Positive c_P^{ex} values were confirmed for both chloride and fluoride eutectic compositions, with values for FLiNaK in agreement with values separately calculated from independently obtained thermal properties. Values were further validated by analysis of the $H_T - H_{298.15}$, reproducing reported values to within 0.75 kJ.mol^{-1} for FLiNaK and ± 1.5 kJ.mol^{-1} for NaCl-$MgCl_2$.

The values/relations for the c_P of the FLiNaK and 58NaCl-42$MgCl_2$ have been appropriately included in MSD-TC. As an example, it will serve to reduce the uncertainty in thermal-hydraulic analysis and reactor safety analysis for MSRs utilizing the salt systems. More generally, the property measurement protocol is readily transferable to the investigation of other molten salts, including actinide-bearing fuels, and establishes a foundation for systematic investigation of wider phenomena such as the effect of oxygen contamination on molten salt properties.

Acknowledgements

This research was supported by the U.S. Department of Energy Office of Nuclear Energy, Advanced Reactor Technology Molten Salt Reactor Program. The authors also recognize the Laboratory Directed Research and Development (LDRD) program at Idaho National Laboratory (INL) under Project No. 22286 for supporting the development of laser welding capabilities at USC.

References

1. Holcomb DE, Cetiner SM (2010) An Overview of Liquid Fluoride Salt Heat Transport Systems

2. Arias I, Cardemil J, Zarza E, Valenzuela L, Escobar R (2022) Latest developments, assessments and research trends for next generation of concentrated solar power plants using liquid heat transfer fluids. Renewable and Sustainable Energy Reviews 168:112844. https://doi.org/10.1016/j.rser.2022.112844

3. Serp J, Allibert M, Beneš O, Delpech S, Feynberg O, Ghetta V, Heuer D, Holcomb D, Ignatiev V, Kloosterman JL, Luzzi L, Merle-Lucotte E, Uhlíř J, Yoshioka R, Zhimin D (2014) The molten salt reactor (MSR) in generation IV: Overview and perspectives. Progress in Nuclear Energy 77:308–319. https://doi.org/10.1016/j.pnucene.2014.02.014

4. Ard J, Johnson K, Christian M, Schorne-Pinto J, Yingling J, Besmann T, Mcmurray J, Peng J (2020) Status Report on the Molten Salt Thermodynamic Database (MSTDB) Development (FY20). Oak Ridge National Laboratory, Oak Ridge, TN, USA

5. Ard JC, Yingling JA, Johnson KE, Schorne-Pinto J, Aziziha M, Dixon CM, Christian MS, McMurray JW, Besmann TM (2022) Development of the Molten Salt Thermal Properties Database − Thermochemical (MSTDB−TC), example applications, and LiCl−RbCl and UF3−UF4 system assessments. Journal of Nuclear Materials 563:153631. https://doi.org/10.1016/j.jnucmat.2022.153631

6. Ard JC, Schorne-Pinto J, Aziziha M, Yingling JA, Mofrad AM, Johnson KE, Dixon CM, Besmann TM (2023) Thermodynamic assessments or reassessments of 30 pseudo-binary and -ternary salt systems. The Journal of Chemical Thermodynamics 177:106931. https://doi.org/10.1016/j.jct.2022.106931

7. Termini N, Birri T, Henderson S, Ezell ND (2023) An Overview of the Molten Salt Thermal Properties Database– Thermophysical, Version 2.1.1 (MSTDB-TP v.2.1.1). Oak Ridge National Laboratory (ORNL), Oak Ridge, TN (United States)

8. Birri A, Chesser R, Termini N, Numbers JC, Garland K, Rose MA (2025) Reference Correlations for the Density and Viscosity of Molten Alkali and Alkaline Earth Fluoride Salts. Journal of Physical and Chemical Reference Data 54:023101. https://doi.org/10.1063/5.0264576

9. Pelton A (2018) Phase Diagrams and Thermodynamic Modeling of Solutions. Elsevier

10. Rogers DJ, Yoko T, Janz GJ (1982) Fusion properties and heat capacities of the eutectic lithium fluoride-sodium fluoride-potassium fluoride melt. J Chem Eng Data 27:366–367. https://doi.org/10.1021/je00029a041

11. Khokhlov V, Korzun I, Dokutovich V, Filatov E (2011) Heat capacity and thermal conductivity of molten ternary lithium, sodium, potassium, and zirconium fluorides mixtures. Journal of Nuclear Materials 410:32–38. https://doi.org/10.1016/j.jnucmat.2010.12.306

12. Lichtenstein T, Rose MA, Krueger J, Wu E, Williamson MA (2020) Thermochemical Property Measurements of FLiNaK and FLiBe in FY 2020. Argonne National Lab. (ANL), Argonne, IL (United States)

13. Yin H, Zhang P, An X, Zhao S, Xie L, Wang W (2016) The effect of corrosion product CrF3 on thermo-physical properties of FLiNaK. Journal of Nuclear Science and Technology 53:61–68. https://doi.org/10.1080/00223131.2015.1026859

14. Minchenko V, Filatov E, Khokhlov V, Korzun I (1999) Temperature and concentration changes of isobaric and isochoric heat capacity of some halide melts (in Russian). Rasplavy (Melts) 13:21–33

15. Ezell ND, Gallagher R, Agca C (2021) Thermal property characterization of Molten Salt Reactor relevant salts

16. An X-H, Cheng J-H, Su T, Zhang P (2017) Determination of thermal physical properties of alkali fluoride/carbonate eutectic molten salt. Abu Dhabi, United Arab Emirates, p 070001

17. Schorne-Pinto J, Aziziha M, Tisdale HB, Mofrad AM, Birri A, Christian MS, Ard JC, Booth RE, Yingling JA, Soldan Palma JP, Dixon C, Loye H-CZ, Besmann TM (2024) Thermal Property Modeling and Assessment of the Physical Properties of FLiNaK. ACS Appl Energy Mater 7:4016–4029. https://doi.org/10.1021/acsaem.4c00321

18. Gardner LD, Dowding EA, Rojas J, Rose MA (2025) Property Measurements of LiF-NaF-KF Molten Salts Doped with Corrosion Products and Oxygen

19. Ivory J, Nielson A, Walton D, Memmott M (2026) Thermophysical property analysis of UF4-FLiNaK molten salt: Density and heat capacity measurements. Progress in Nuclear Energy 192:106157. https://doi.org/10.1016/j.pnucene.2025.106157

20. Ambrosek JW (2011) Molten Chloride Salts for Heat Transfer in Nuclear Systems. Ph.D. thesis, University of Wisconsin-Madison

21. Rose M, Krueger J, Lichtenstein T, Wu E, Gardner L (2021) Precision of Property Measurements with Reference Molten Salts

22. Rudenko A, Redkin A, Il'ina E, Pershina S, Mushnikov P, Zaikov Y, Kumkov S, Liu Y, Shi W (2022) Thermal Conductivity of FLiNaK in a Molten State. Materials 15:5603. https://doi.org/10.3390/ma15165603

23. Powers WD, Blalock GC (1956) Enthalpies and heat capacities of solid and molten fluoride mixtures

24. Filatov ES (1985) Thermal conductivity, thermal diffusivity and heat capacity at constant pressure of molten alkali metal fluorides and their mixtures (in Russian). Academy of Sciences of the Soviet Union - Ural Scientific Center

25. Kosaka M, Asahina T, Taoda H, Kishi A (1982) Heat of Fusion and Heat Capacity of MX and M2Y (M = Li, Na, K, : X = NO3, F, Cl : Y = CO3, SO4) Ternary Eutectic Salts (in Japanese). Nippon Kagaku Kaishi 6:977–982

26. Munro T, Chiu R, Rose MA, Benes O, Boca M, Gardner DN, Leong A, Mastromarino S, Pamplin KL, Piro MHA, Saoudi M, Schorne-Pinto J, Sclafani CM, Smith AL, Smith ND, Sulejmanovic D, Berry AM, Chen R, Chung KM, Dahman C, Detrick K, Feng T, Ocádiz Flores JA, Gallagher R, Gardner L, Guo X, Jackson JM, Karlsson T, Kasper P, Kim H, McIlwain L, Memmott M, Merritt B, Monreal MJ, Oishi K, Orlovskaya L, Parker SS, Prudil AA, Robison AD, Scott S, Romero RC, Vlieland J, Woods ME, Zhang J, Besmann TM, Scarlat RO (2025) Round Robin Measurements of Molten Salt Properties for LiF-NaF-KF (FLiNaK) and NaCl-KCl Mixtures. J Chem Eng Data acs.jced.5c00421. https://doi.org/10.1021/acs.jced.5c00421

27. Karlsson TY, Middlemas SC, Nguyen M-T, Woods ME, Tolman KR, Glezakou V-A, Herrmann SD, Schorne-Pinto J, Johnson RD, Reddish SE, Warmann SA, Paviet PD (2023) Synthesis and thermophysical property determination of NaCl-PuCl3 salts. Journal of Molecular Liquids 387:122636. https://doi.org/10.1016/j.molliq.2023.122636

28. Piro MHA, Lipkina K, Hallatt D (2021) Exploring crucible designs for differential scanning calorimetry measurements of fluoride salts. Thermochimica Acta 699:178860. https://doi.org/10.1016/j.tca.2021.178860

29. Muñoz-Sánchez B, Nieto-Maestre J, Imbuluzqueta G, Marañón I, Iparraguirre-Torres I, García-Romero A (2017) A precise method to measure the specific heat of solar salt-based nanofluids. J Therm Anal Calorim 129:905–914. https://doi.org/10.1007/s10973-017-6272-x

30. Lonergan J, Goncharov V, Swinhart M, Makovsky K, Rollog M, McNamara B, Clark R, Cutforth D, Armstrong C, Guo X, Paviet P (2023) Thermodynamic investigation of the NaCl-KCl salt system from 25 to 950 °C. Journal of Molecular Liquids 391:122591. https://doi.org/10.1016/j.molliq.2023.122591

31. Strzelecki AC, Cockreham CB, Parker SS, Mann SC, Lhermitte C, Wu D, Guo X, Monreal M, Jackson JM, Mitchell J, Boukhalfa H, Xu H (2024) A new methodology for measuring the enthalpies of mixing and heat capacities of molten chloride salts using high temperature drop calorimetry. Review of Scientific Instruments 95:014103. https://doi.org/10.1063/5.0144910

32. Beneš O, Konings RJM, Kuenzel C, Sierig M, Dockendorf A, Vlahovic L (2009) The high-temperature heat capacity of the (Li, Na)F liquid solution. The Journal of Chemical Thermodynamics 41:899–903. https://doi.org/10.1016/j.jct.2009.02.009

33. Scharrer M, Bonatti L, Geraci T, Ushakov SV, Majzlan J, Bustamante M, Kojitani H, Guo X, Xu H, Zhang L, Lilova K, Hayun S, Subramani T, Navrotsky A (2025) The joys and jitters of high-temperature calorimetry. J Am Ceram Soc 108:e20381. https://doi.org/10.1111/jace.20381

34. Joint Committee for Guides in Metrology (2008) JCGM 100:2008, Evaluation of measurement data — Guide to the expression of uncertainty in measurement (GUM 1995 with minor corrections)

35. Foster KR, Schorne-Pinto J, Booth RE, Husek A, Aziziha M, Tisdale HB, Fitzpatrick BWN, Zur Loye H-C, Piro MHA, Besmann TM (2025) Purification of uranium tetrafluoride using ammonium bifluoride. Journal of Fluorine Chemistry 285–286:110449. https://doi.org/10.1016/j.jfluchem.2025.110449

36. Gaune-Escard M, Bogacz A, Rycerz L, Szczepaniak W (1996) Heat capacity of LaCl3, CeCl3, PrCl3, NdCl3, GdCl3, DyCl3. Journal of Alloys and Compounds 235:176–181. https://doi.org/10.1016/0925-8388(95)02071-3

37. Gaune-Escard M, Rycerz L (1999) Heat Capacity of K3LnCl6 Compounds with Ln = La, Ce, Pr, Nd. Zeitschrift für Naturforschung A 54:229–235. https://doi.org/10.1515/zna-1999-3-412

38. Rycerz L, Ingier-Stocka E, Golonka-Cieślak M, Gaune-Escard M (2003) Thermal and conductometric studies of NdBr3 and NdBr3-LiBr binary system. Journal of Thermal Analysis and Calorimetry 72:241–251. https://doi.org/10.1023/A:1023940324328

39. Rycerz L, Gaune-Escard M (1999) Heat Capacity of the Rb3LnCl6 Compounds with Ln = La, Ce, Pr, Nd. Zeitschrift für Naturforschung A 54:397–403. https://doi.org/10.1515/zna-1999-6-709

40. Della Gatta G, Richardson MJ, Sarge SM, Stølen S (2006) Standards, calibration, and guidelines in microcalorimetry. Part 2. Calibration standards for differential scanning calorimetry* (IUPAC Technical Report). Pure and Applied Chemistry 78:1455–1476. https://doi.org/10.1351/pac200678071455

41. Höhne GWH, Hemminger WF, Flammersheim H-J (2003) Differential Scanning Calorimetry. Springer, Berlin, Heidelberg

42. Benigni P, Mikaelian G, Pothin R, Berche A, Ayral RM, Tedenac JC, Jund P, Rogez J (2016) Measurement of the heat capacity of ZnSb by DSC between 300 and 673 K. Calphad 55:238–242. https://doi.org/10.1016/j.calphad.2016.09.008

43. Schorne-Pinto J, Janghorban A, Lomello-Tafin M, Pisch A, Mikaelian G, Benigni P, Barnabé A, Cassayre L (2019) Assessment of thermodynamic data for CuCrO2 delafossite from calorimetric measurements. Thermochimica Acta 680:178345. https://doi.org/10.1016/j.tca.2019.178345

44. Dinsdale AT (1991) SGTE data for pure elements. Calphad 15:317–425. https://doi.org/10.1016/0364-5916(91)90030-N

45. Ditmars DA, Ishihara S, Chang SS, Bernstein G, West ED (1982) Enthalpy and Heat-Capacity Standard Reference Material: Synthetic Sapphire (Alpha-Al2O3) From 10 to 2250 K. J RES NATL BUR STAN 87:159. https://doi.org/10.6028/jres.087.012

46. Archer DG (1993) Thermodynamic Properties of Synthetic Sapphire (α-Al2O3), Standard Reference Material 720 and the Effect of Temperature-Scale Differences on Thermodynamic Properties. Journal of Physical and Chemical Reference Data 22:1441–1453. https://doi.org/10.1063/1.555931

47. Markov BF, Tishura TA, Budarina AN (1981) Enthalpy of formation of crystallized melts of the NaCl-MgCl2 system. Ukrainskil Khimicheskii Zhurnal 47:696–697

48. Denielou, L, Petitet J P, Tequi C (1980) Calorimetric study of MgCl2-NaCl mixtures. Revue generale de thermique 19:303–309

49. Gowtham Mohan, Mahesh Venkataraman, Judith Gomez-Vidal, Joe Coventry (2018) Assessment of a novel ternary eutectic chloride salt for next generation high-temperature sensible heat storage. Energy Conversion and Management 167:156–164

50. Williams DF (2006) Assessment of Candidate Molten Salt Coolants for the NGNP/NHI Heat-Transfer Loop

51. Wang X, Rincon JD, Li P, Zhao Y, Vidal J (2021) Thermophysical Properties Experimentally Tested for NaCl-KCl-MgCl2 Eutectic Molten Salt as a Next-Generation High-Temperature Heat Transfer Fluids in Concentrated Solar Power Systems. Journal of Solar Energy Engineering 143:041005. https://doi.org/10.1115/1.4049253

52. Zhao Y (2020) Molten Chloride Thermophysical Properties, Chemical Optimization, and Purification

53. Padinhare Manissery A, Schorne-Pinto J, Zhoujin Y, Wisesa P, Booth RE, Tisdale HB, Wilson JA, Paz Soldan Palma J, Gardiner ZK, Karlsson TY, zur Loye H-C, Besmann TM (2026) Elucidating the Thermodynamics and Phase Equilibria of the NaCl−MgCl2 System (Manuscript submitted for publication)

Supplementary Files

This is a list of supplementary files associated with this preprint. Click to download.

- MethodforMeasuringtheSpecificHeatCapacityofMoltenSaltsSI.docx